Supplementary Material

METHODS

***Preparation of ApoA-I Mutants*.** To create the cDNA for the domain-swap human-M apoA-I and mouse-H apoA-I proteins, WT human and WT mouse apoA-I cDNA in a pet32 vector were engineered using the Stratagene "domain-swap" protocol where the domain to be swapped was first PCR-amplified, gel purified and then used as a megaprimer in the subsequent QuickChange site-directed mutagenesis (1). To express the apoA-I variants the cDNA of interest was cloned into the multiple cloning sites of the pET32a (+) vector, and the target protein was expressed as a histidine-tagged fusion protein with the 109-amino acid thioredoxin (Trx) at the amino terminus (2,3). The resulting plasmids were transformed into *Escherichia coli* strain BL21(DE3). These transformed cells were cultured in LB medium at 37˚C and expression of the fusion protein Trx-apoA-I was induced with isopropyl-β-D-thiogalactopyranoside for 3 h. After sonicating the bacterial pellet, the lysate was centrifuged and the supernatant loaded onto a nickel-chelating, histidine-binding resin column (Novagen). The Trx-apoA-I fusion protein bound to the column was eluted, pooled, and dialyzed against 20 mM NH_4HCO_3. Subsequently, the fusion protein was complexed with dimyristoyl phosphatidylcholine (DMPC) to prevent non-specific cleavage, and then cleaved with thrombin to release the Trx. The mixture was then lyophilized, delipidated, and dissolved in 6 M guanidine hydrochloride (GdnHCl) solution. Trx was separated from apoA-I by gel filtration chromatography on a Sephacryl S-300 column. Further purification (>95%) of the proteins was done by gel filtration with Superdex 75 and/or anion exchange chromatography with Q-Sepharose. Purity was confirmed by SDS-PAGE (1,4). All proteins were stored at -80˚C in lyophilized form and before use were dissolved in the appropriate buffer containing 6M GdnHCl and dialyzed extensively before use.

***Preparation of ApoA-I Adeno-Associated Virus (AAV)*.** To create the cDNA for the domain-swap human-M apoA-I and mouse-H apoA-I proteins, WT human and WT mouse apoA-I cDNA in a pAAV vector were engineered using the Stratagene "domain-swap" protocol where the

domain to be swapped was first PCR-amplified, gel purified and then used as a megaprimer in the subsequent QuickChange site-directed mutagenesis (1). After the PCR reaction the sample was digested with Dpn I, an endonuclease specific for methylated and hemimethylated DNA, to digest the parental DNA template and select for mutation-containing synthesized DNA. The purified mutant plasmid was then transformed into XL1-Blue supercompetent cells. Several colonies were isolated and used to inoculate Luria-Bertani media containing 100mg/ml ampicillin. The resulting plasmids were sequenced and restriction digested to confirm the presence of the intended mutation. The plasmid containing the mutant sequence was then submitted to the University of Pennsylvania Vector Core for use in creating the apoA-I AAV, serotype 8 (5).

Liver mRNA levels. Total RNA was isolated from mouse livers using an EZ1 RNA mini kit (Qiagen) according to the manufacturer's instructions. 0.1-1.0 µg of total RNA was reverse transcribed using iScript (BioRad). Quantitative real-time PCR analysis was performed using primers for human (hs00163641_m1) and mouse (mm00437569_m1) apoA-I from Applied Biosciences. The relative quantities of mRNA were determined using the method of comparative changes in threshold cycle and data are expressed as fold change (± SD) relative to mouse β-actin.

Quantification of ApoA-I Levels. The concentrations of the various apoA-I variants in mouse plasma were determined by running triplicate plasma samples (1 µl) from the apoA-I-expressing mice on 4-12% SDS-PAGE tris-glycine gels (Invitrogen) along with lanes containing different amounts of the appropriate recombinant apoA-I. The gel were then stained for protein with Coomassie blue and digitally imaged. The concentrations of the apoA-I variants were then determined by spot densitometry (ImageJ) and comparison to the standard curve.

Non-Denaturing Gradient Gel Electrophoresis. Isolated HDL were run at 4˚C using 4-20% tris-glycine gels (Invitrogen) in a Tris (170mM), boric acid (80mM), EDTA (15 mM) and sodium azide (15mM) running buffer. Gels were run for 1800 volt/h to equilibrium.

Macrophage RCT Studies. RCT studies were performed as previously described (5-10). J774 cells were grown in suspension in RPMI 1640 medium supplemented with 10% fetal bovine serum. Cells were radiolabeled with 5 µCi/mL [^{3}H]cholesterol and cholesterol enriched with 100 µg/mL of acetylated LDL for 48 h. These labeled foam cells were washed twice, equilibrated in medium with 0.2% bovine serum albumin for 6 h, spun down and resuspended in RPMI medium immediately before use.

Experiments were performed in male apoA-I-null C57/Bl6 mice obtained from Jackson Labs. All mice were fed a standard chow diet. For each experiment, 30 mice (n = 6/group) received intraperitoneal (IP) injections of 1 X 10^{12} GC of AAV8 WT human apoA-I, WT mouse apoA-I, human-M apoA-I, mouse-H apoA-I or LacZ . On day 70 after vector injection, animal received ip injections of [^{3}H]cholesterol-labeled J774 cells as previously described (6) and were caged individually with unlimited access to food and water. Blood was collected at 6, 24, and 48 hours, and the plasma was used for liquid scintillation counting (LSC). Feces were collected continuously from 0 to 48 h and stored at 4 ˚C before being counted. At 48 hours after injection mice were exsanguinated. The total feces collected were weighed and soaked in deionized water (1 mL water per 100 mg feces) overnight at 4 ˚C. An equal volume of ethanol was added the next day and samples were homogenized with 200 µL of the homogenized samples counted in an LSC in duplicate.

Endogenous LCAT Assay. Endogenous LCAT cholesterol esterification rate (CER) in whole plasma was measured using a modified Stokke and Norum procedure (11,12). A tracer amount of [^{3}H]cholesterol in toluene was added into a 50 mg/mL bovine serum albumin (BSA) solution, and the toluene was evaporated under N_2. Seventy five microliters of plasma were incubated with the BSA solution containing 3 X 10^6 dpm of [^{3}H]cholesterol on ice overnight to allow the [^{3}H]cholesterol tracer to equilibrate evenly across the entire spectrum of lipoproteins. The sample was diluted to 300 µL with 0.2 M phosphate buffer (pH 7.4) and divided into three aliquots. Two aliquots were incubated at 37 ˚C for 30 min as duplicates, while the remaining

aliquot was maintained at 4 ˚C as a control. All subsequent procedures were the same as described previously (13). Briefly, after incubation, the samples were placed on ice, and the lipid was extracted by the Bligh/Dyer method. The extracted lipids were subjected to TLC using a neutral solvent system to separate the FC and CE radio label which was quantified by scintillation counting. Endogenous LCAT activity was expressed as percentage of FC esterified (calculated as CE/(CE+FC)) and as nanomoles of CE formed per milliliter of plasma (calculated as plasma FC concentration X (%FC esterified/100%) during the 30 min incubation.

Exogenous LCAT Assay. The LCAT reaction was monitored by following the conversion of radiolabeled cholesterol ester using palmitoyl-oleoyl phosphatidylcholine (POPC) rHDL (rHDL containing either WT or mutant apoA-I were made using the sodium cholate dialysis method (14)) as previously described (13). The complexes were assayed in triplicate using 0-2 µg/ 0.5 mL of substrate cholesterol in a final concentration of 10 mM Tris, pH. 7.4, 140 mM NaCL, 0.25 mM EDTA, 0.15 sodium azide, 0.6% fatty acid-free bovine serum albumin, 2 mM DTT, and 20-40 ng of recombinant human His-tag LCAT (15). The reactions were carried out over 10-40 min at 37˚C and the conversion of [^{3}H]cholesterol to [^{3}H]cholesterol ester was determined after lipid extraction of the incubation mixture followed by thin-layer chromatography. The extent of cholesterol esterification was kept below 15% and the fractional cholesterol esterification rate was expressed as nanomoles of cholesterol ester formed per hour per nanogram of LCAT. Apparent V_{max} and K_m values were determined by fitting the data to the Michaelis-Menten equation (Graphpad Prism).

Cellular Cholesterol Efflux. J774 macrophages were grown in RPMI 1640 medium containing 10% FBS + 50 µg/mL gentamycin and incubated at 37 ˚C in a humidified chamber. For efflux experiments, these cells were then seeded in 12-well tissue culture plates and grown to 80-90% confluence. The following day wells were washed with MEM-HEPES. The final wash was removed and media containing 1% FBS + [^{3}H]cholesterol (1 µCi/mL) + CP-113 818 (2 µg/mL), an ACAT inhibitor, was added for 24 hours. After this, cells were incubated in media containing

0.2% BSA for 18 hours to allow cellular cholesterol radiolabel to equilibrate. To up-regulate the expression of ABCA1, some incubations also contained 0.3 mmol/L CTP-cAMP. After equilibration, time zero cells were harvested to determine total cpm, protein and FC mass in the cells before the acceptors were added. To initiate cholesterol efflux, media containing 0-20µg/mL of apoA-I variant as acceptor was added. Media were sampled at 4 h, filtered, and counted by LSC to determine the [^{3}H] released. The percent FC efflux was calculated after subtracting the background FC efflux (without apoA-I) as follows: (counts/min in medium at 4 h/cpm in cells at t = 0) X 100. K_m and V_{max} values were calculated by fitting the fractional lipid efflux values obtained at 4 h and different concentrations of apoA-I to the Michaelis-Menten equation (Graphpad Prism) .

BHK cells expressing ABCG1 were plated for a day and then labeled for 24 h with 3 µCi/ml of [^{3}H] free cholesterol in the presence of 2.5 % FBS. Cells were later treated with or without mifepristone for 18 h in DMEM containing 0.2% BSA. Efflux of FC was induced by incubation with HDL acceptors for 4 h. Efflux was calculated by measuring the release of radiolabeled FC into the medium, as previously described (16). All of the experiments were performed in the presence of the ACAT inhibitor CP113818.

Cholesterol Influx to Cells. Rat Fu5AH hepatoma cells were prepared as described previously (17) and incubated with 20% serum containing [^{3}H]cholesterol and [^{3}H]cholesteryl ester that was obtained from mice expressing the apoA-I variants and treated with [^{3}H]cholesterol-labeled macrophages for the RCT assay. After 6 h, the cells were washed three times with PBS, the cell lipids were extracted with isopropyl alcohol as previously described (18) and the levels of [^{3}H] label determined. Fu5AH cells were pretreated either with or without Block Lipid Transport-1 (BLT-1) (19) for 2 h to inhibit any transport of cholesterol from HDL to the cells via SR-BI.

Data Analysis. Data are from representative experiments and are expressed as mean ± SD. Statistical test for significance was done using an unpaired t-test or 1 way Anova.

Supplementary Results

The primary structures of WT mouse and WT human apoA-I molecules are very similar, with a 65% identity (20). The most highly differentiated part of WT human and WT mouse apoA-I is the C-terminal domain which is only 46% identical. These differences in amino acid sequence result in differences in polarity between human and mouse apoA-I with an average hydrophathic index per amino acid residue of -0.84 and -0.95 for WT human and WT mouse apoA-I, respectively (21); a more negative index value indicates a more polar molecule. Both human and mouse apoA-I adopt a two-domain tertiary structure with an N-terminal helix bundle domain and a separately folded C-terminal domain (1). The hydropathies of the human and mouse N-terminal domains are very similar, but, the mouse C-terminal domain is highly polar compared to the human C-terminal domain (-0.72 and -0.3, respectively). This difference in domain polarity has important consequences for the functionalities of the apoA-I molecules.

Physical biochemical measurements showed that WT human and WT mouse apoA-I had very different stabilities based on their susceptibilities to thermal and Gdn HCl denaturation (Supplementary Table I). For instance the human N-terminal helix bundle (residues 1-189) was much more stable than the mouse N-terminal helix bundle domain (residues 1-186) as indicated by the 15˚C difference in melting temperature. In addition to the differences in polarities of the human and mouse apoA-I C-terminal domains, the results in the Supplementary Table I demonstrate that there were significant differences in secondary structure and stability. The mouse C-terminal domain had very low helicity in dilute solution whereas the human C-terminal domain was partially α-helical and underwent cooperative thermal denaturation. Fluorescence spectroscopy measurements of ANS binding indicated that WT human apoA-I had more hydrophobic surface exposure compared to WT mouse apoA-I (Supplementary Table I). The hydrophobic surface exposure in both the human and mouse N-terminal helix bundle domains are similar, but the mouse C-terminal domain had much less hydrophobic surface exposed than

the human counterpart. This difference arises from the higher polarity of the mouse C-terminal domain.

Regarding the ability to interact with lipids, the catalytic efficiencies for DMPC clearance (Supplementary Table I) showed that, relative to the WT human apoA-I molecule, the human N-terminal domain did not clear DMPC MLV effectively while the C-terminal domain did. Thus, the stable helix bundle domain did not interact well with lipid surfaces in contrast to the hydrophobic C-terminal domain that interacted with high affinity. These data are in agreement with the two step model of lipid binding where the initial interaction occurs with the C-terminal α-helix ,which is accompanied by an increase in α-helix content in the C-terminal domain (2). In the second step the N-terminal helix bundle opens allowing the amphipathic α-helices to interact with lipids. The two-step model describes the binding of human apoA-I to a lipid surface, but it does not describe the situation for mouse apoA-I. The highly polar C-terminal domain of mouse apoA-I does not interact with lipid surfaces and did not solubilize DMPC MLV. However, the relatively unstable mouse N-terminal helix bundle bound well to lipid surfaces and exhibited a catalytic efficiency of 0.30 for clearance of DMPC (Supplementary Table I). Based on these data it would be expected that a hybrid protein comprised of the mouse N-terminal domain and the hydrophobic human C-terminal domain would interact with lipid surfaces in a very efficient manner. This hypothesis was proven correct; the mouse-H apoA-I hybrid was the most efficient apoA-I variant at solubilizing DMPC MLV exhibiting a catalytic efficiency of 0.36 (Supplementary Table 1). Conversely, the human-M apoA-I hybrid, which was comprised of the stable, low lipid affinity human N-terminal helix bundle domain and the polar mouse C-terminal domain was very inefficient at solubilizing DMPC MLV (catalytic efficiency 0.16).

1. Tanaka M, Koyama M, Dhanasekaran P, Nguyen D, Nickel M, Lund-Katz S, Saito H, and Phillips MC. Influence of tertiary structure domain properties on the functionality of apolipoprotein A-I. *Biochemistry.* 2008;47: 2172-2180.
2. Saito H, Dhanasekaran P, Nguyen D, Holvoet P, Lund-Katz S, and Phillips MC. Domain structure and lipid interaction in human apolipoproteins A-I and E, a general model. *J. Biol. Chem.* 2003;278: 23227-23232.
3. Morrow JA, Arnold KS, and Weisgraber KH. Functional characterization of apolipoprotein E isoforms overexpressed in *Escherichia coli*. *Protein Expr.Purif.* 1999;16: 224-230.
4. Koyama M, Tanaka M, Dhanasekaran P, Lund-Katz S, Phillips MC, and Saito H. Interaction between the N- and C-terminal domains modulates the stability and lipid binding of apolipoprotein A-I. *Biochemistry.* 2009;48: 2529-2537.
5. Tanigawa H, Billheimer JT, Fuki I, Thoyama JC, Rothblat G, and Rader DJ. AAV8-mediated overexpression of lecithin-cholesterol acyltransferase fails to promote macrophage reverse cholesterol transport in vivo. *Circulation.* 2007;116: 197-197.
6. Zhang Y, Zanotti I, Reilly MP, Glick JM, Rothblat GH, and Rader DJ. Overexpression of apolipoprotein A-I promotes reverse transport of cholesterol from macrophages to feces in vivo. *Circulation.* 2003;108: 661-663.
7. Zhang YZ, Da Silva JR, Reilly M, Billheimer JT, Rothblat GH, and Rader DJ. Hepatic expression of scavenger receptor class B type I (SR-BI) is a positive regulator of macrophage reverse cholesterol transport in vivo. *J. Clin. Invest.* 2005;115: 2870-2874.
8. Moore RE, Navab M, Millar JS, Zimetti F, Hama S, Rothblat GH, and Rader DJ. Increased atherosclerosis in mice lacking apolipoprotein A-I attributable to both impaired reverse cholesterol transport and increased inflammation. *Circ. Res.* 2005;97: 763-771.

9. Naik SU, Wang X, Da Silva JS, Jaye M, Macphee CH, Reilly MP, Billheimer JT, Rothblat GH, and Rader DJ. Pharmacological activation of liver X receptors promotes reverse cholesterol transport in vivo. *Circulation.* 2006;113: 90-97.

10. Wang X, Collins HL, Ranalletta M, Fuki IV, Billheimer JT, Rothblat GH, Tall AR, and Rader DJ. Macrophage ABCA1 and ABCG1, but not SR-BI, promote macrophage reverse cholesterol transport in vivo. *J. Clin. Invest.* 2007;117: 2216-2224.

11. Stokke KT, and Norum KR. Determination of lecithin - cholesterol acyltransfer in human blood plasma. *Scand. J. Clin. Lab. Invest.* 1971;27: 21-&.

12. Zhao Y, Thorngate FE, Weisgraber KH, Williams DL, and Parks JS. Apolipoprotein E is the major physiological activator of lecithin-cholesterol acyltransferase (LCAT) on apolipoprotein B lipoproteins. *Biochemistry.* 2005;44: 1013-1025.

13. Alexander E, Bhat S, Thomas M, Weinberg R, Cook V, Bharadwaj M, and Sorci-Thomas M. Apolipoprotein A-I helix 6 negatively charged residues attenuate lecithin-cholesterol acyltransferase (LCAT) reactivity. *Biochemistry.* 2005;44: 5409-5419.

14. Jonas AJ, Kezdy KE, and Wald JH. Defined apoliporpotein A-I conformations in reconstituted high density lipoprotein discs. *J. Biol. Chem.* 1989;264: 4818-4824.

15. Chisholm JW, Gebre AK, and Parks JS. Characterization of C-terminal histidine-tagged human recombinant lecithin:cholesterol acyltransferase. *J. Lipid Res.* 1999;40: 1512-1519.

16. Sankaranarayanan S, Oram JF, Asztalos BF, Vaughan AM, Lund-Katz S, Adorni MP, Phillips MC, and Rothblat GH. Effects of acceptor composition and mechanism of ABCG1-mediated cellular free cholesterol efflux. *J. Lipid Res.* 2008;50: 275-284.

17. Zimetti F, Weibel GK, Duong M, and Rothblat GH. Measurement of cholesterol bidirectional flux between cells and lipoproteins. *J. Lipid Res.* 2006;47: 605-613.

18. Yancey PG, De la Llera-Moya M, Swarnakar S, Monzo P, Klein SM, Connelly MA, Johnson WJ, Williams DL, and Rothblat GH. High density lipoprotein phospholipid

composition is a major determinant of the bi-directional flux and net movement of cellular free cholesterol mediated by scavenger receptor BI. *J. Biol. Chem.* 2000;275: 36596-36604.

19. Nieland TJF, Penman M, Dori L, Krieger M, and Kirchhausen T. Discovery of chemical inhibitors of the selective transfer of lipids mediated by the HDL receptor SR-BI. *Proc Natl Acad Sci USA.* 2002;99: 15422-15427.

20. Brouillette CG, Anantharamaiah GM, Engler JA, and Borhani DW. Structural models of human apolipoprotein A-I: a critical analysis and review. *Biochim. Biophys. Acta.* 2001;1531: 4-46.

21. Kyte J, and Doolittle RF. A Simple Method for Displaying the Hydropathic Character of a Protein. *J. Mol. Biol.* 1982;157: 105-132.

22. Liu L, Bortnick AE, Nickel M, Dhanasekaran P, Subbaiah PV, Lund-Katz S, Rothblat GH, and Phillips MC. Effects of apolipoprotein A-I on ATP-binding cassette transporter A1-mediated efflux of macrophage phospholipid and cholesterol: formation of nascent high density lipoprotein particles. *J. Biol. Chem.* 2003;278: 42976-42984.

Supplementary Figure I. Quantitative analysis of human apoA-I mRNA from mouse livers 6 weeks post AAV injection. Total RNA was extracted from mouse livers and analyzed by real time PCR as described in Methods. Data are expressed as fold difference (± SD) relative to mouse β-actin and are normalized to the value for WT human apoA-I.

Supplementary Figure II. Gel filtration elution profiles of serum samples collected from mice used in macrophage RCT experiments. Serum samples from mice expressing WT H, WT M, H-M and M-H apoA-I were collected during the 48 h bleed (Figure 2A) and the labeled lipoprotein particles were separated by gel filtration chromatography on a calibrated Superdex 200 column (22). Fractions were collected and radioactivity was determined by liquid scintillation counting. The elution volumes for particles of defined hydrodynamic diameter are indicated by the arrows in the top panel.

Supplementary Figure III. Exogenous LCAT assay. rHDL (0.125 µg - 2.0 µg cholesterol) radiolabled with [^{3}H]cholesterol were incubated at 37 ˚C for 10 – 40 min with human LCAT. LCAT activity was determined as described in "Materials and Methods" and is expressed as nanomole of CE formed per hour per milliliter of LCAT [nmol of CE/h/ng LCAT]. (■) WT human apoA-I, (▼) WT mouse apoA-I, (●) Human-M apoA-I, (□) Mouse-H apoA-I.

Supplementary Figure IV. Selective uptake of cholesterol from rHDL containing the apoA-I variants. Rat Fu5AH cells expressing SR-BI were incubated with [^{3}H]cholesterol-labeled rHDL made with the apoA-I variants. After 8h the cell lipids were extracted and the level of [^{3}H]cholesterol label was determined. * = $p \leq 0.0001$.

Supplementary Figure V. Particle size of POPC rHDL. ApoA-I/POPC rHDL were generated by the sodium cholate dialysis method. 10 µg of total rHDL protein was loaded on a 4-20% Tris-Glycine non-denaturing gradient gel and stained with Coomassie brilliant blue. Lanes: (1) WT Human apoA-I, (2) WT Mouse apoA-I, (3) Human-M apoA-I, (4) Mouse-H apoA-I.

Supplementary Figure I

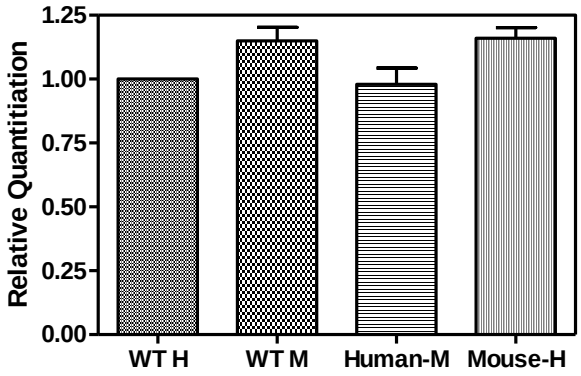

Supplementary Figure II

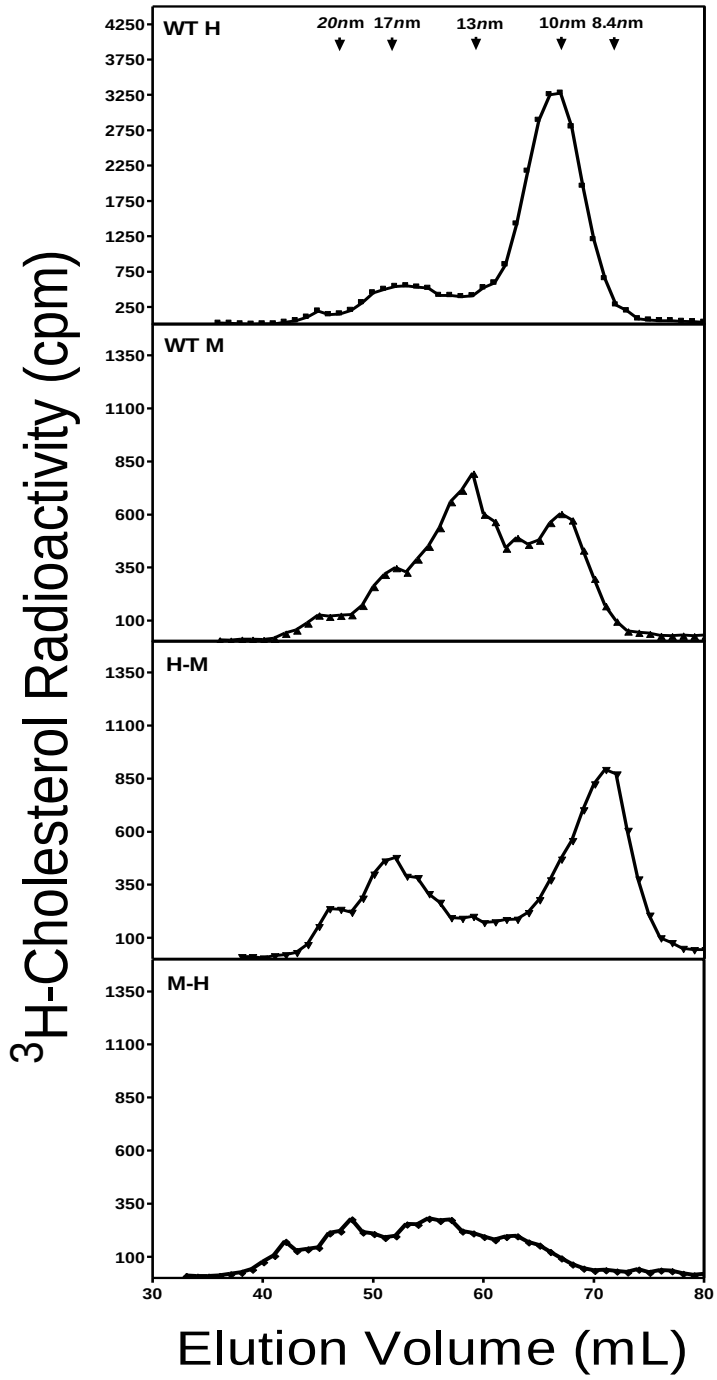

Supplementary Figure III

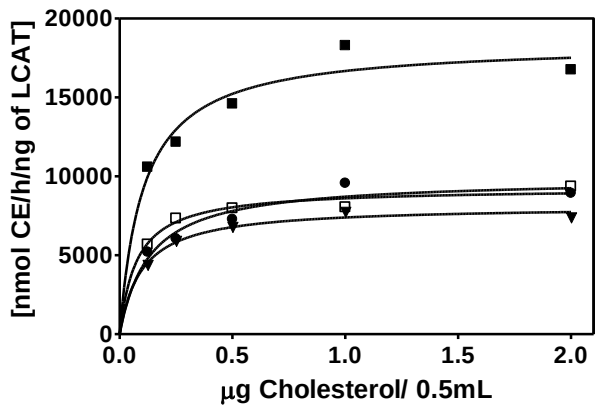

Supplementary Figure IV

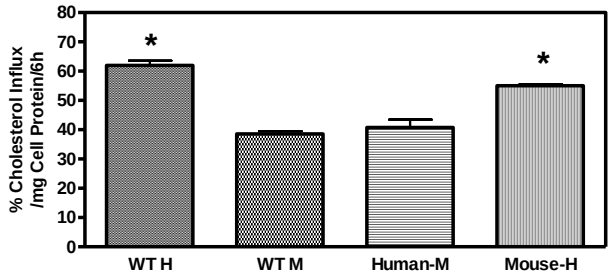

Supplementary Figure V

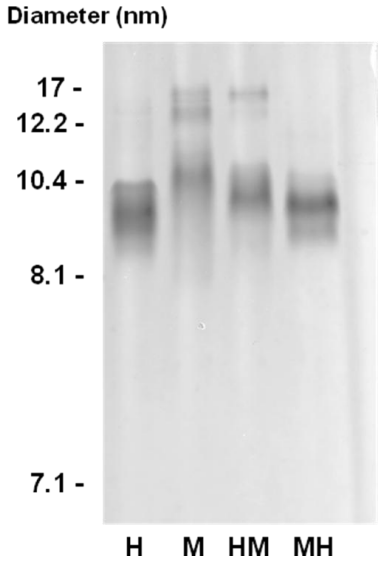

Supplementary Table I: Stabilities and Lipid-Binding Properties of N- and C-Terminal Domains of Human and Mouse ApoA-I[a]							
	structure		stability		Lipid interaction:DMPC clearance[f]		
apoA-I	α-helix[b] (%)	ANS fluorescence intensity[c]	T_m (˚C)[d]	ΔG˚ (kcal/ mol)[e]	K_m (μM)	V_{max} (10 min fractional decrease in A_{325})	Catalytic Efficiency (V_{max}/K_m)
human WT	44 ± 4	1.0	60	3.1 ± 0.3	1.9 ± 0.1	0.60 ± 0.01	0.32
human (1-189)	51 ± 2	0.6	56	3.4 ± 0.1	6.0 ± 0.6	0.47 ± 0.02	0.08
human (190-243)	33 ± 3	1.1	51	-	2.6 ± 0.3	0.54 ± 0.02	0.20
mouse WT	36 ± 5	0.85	45	2.0 ± 0.1	2.8 ± 0.4	0.45 ± 0.02	0.16
mouse (1-186)	37 ± 3	0.7	41	1.9 ± 0.1	2.3 ± 0.1	0.68 ± 0.01	0.30
mouse (187-240)	14 ± 1	0.3	-	-	-	-	-
human-M	45 ± 2	0.8	54	2.3 ± 0.1	5.3 ± 0.5	0.70 ± 0.04	0.16
mouse-H	39 ± 2	1.6	50	2.4 ± 0.1	1.7 ± 0.3	0.62 ± 0.04	0.36

[a]Taken from (1,4). [b]Mean ± SD measured by CD at 50 μg/mL. [c]Values are measured at 50 μg protein/mL and are ratios to WT apoA-I. Error is within 0.1. [d]Midpoint of thermal denaturation measured by CD (±1.5 ˚C). [e]Free energy of denaturation by guanidine HCl as measured by Trp fluorescence which measures the helix bundle stability. [f]Kinetic parameters for solubilization of dimyristoylphosphatidylcholine (DMPC) multilamellar vesicles (MLV). Mean ± SE.

Supplementary Table II: Kinetic Parameters for ABCA1-Mediated Cholesterol Efflux from J774 Cells to ApoA-I Variants			
ApoA-I	Relative V_{max}[a]	K_m (µg apoA-I/mL)	Relative catalytic efficiency[b]
WT Human	1.0	5.7 ± 0.2	1.0
WT Mouse	2.5 ± 0.04	24 ± 0.6	0.6
Human-M	1.6 ± 0.1	9.6 ± 1.3	0.9
Mouse-H	1.3 ± 0.06	3.5 ± 0.5	2.1

[a]The cellular cholesterol released from J774 cells to 20 µg/mL of WT human apoA-I was 9 ± 3%/4 h (n=21) (mean ± SD), and all V_{max} values are normalized to this value.
[b] The catalytic efficiency (V_{max}/K_m) for WT human apoA-I-mediated efflux from J774 cells was 1.6 ± 0.5% cholesterol efflux $(4h)^{-1}(\mu g\ apoA\text{-}I/mL)^{-1}$ (mean ± SD) and all catalytic efficiencies are normalized to this value.

Supplementary Table III: Composition of HDL Isolated from Serum[a]				
AAV	Percent by Weight			
	Phospholipid	Total Cholesterol	Triglyceride	Protein
WT Human	34[b]	31	6	29
WT Mouse	18	54	4	24
Human-M	33	38	3	26
Mouse-H	17	68	1	15
LacZ	15	67	2	16

[a] HDL were isolated via ultracentrifugation from serum take from mice infected with the indicated AAV.

[b] All values represent an average from 1-3 separate experiments run in triplicate with a standard deviation of ± 5%.